3C-SiC nanocrystals/TiO_2 nanotube heterostructures with enhanced photocatalytic performance

J. Zhang,[1] L. Z. Liu,[1] L. Yang,[1] Z. X. Gan,[1] X. L. Wu,[1,a)] and Paul K. Chu[2,a)]
[1]*Key Laboratory of Modern Acoustics, MOE, Institute of Acoustics, and National Laboratory of Solid State Microstructures and Department of Physics, Nanjing University, Nanjing 210093, People's Republic of China*
[2]*Department of Physics and Materials Science, City University of Hong Kong, Tat Chee Avenue, Kowloon, Hong Kong, China*

(Received 27 April 2014; accepted 27 May 2014; published online 9 June 2014)

p-type ultrathin 3C-SiC nanocrystals are coated on heat-treated *n*-type TiO_2 nanotube arrays formed by electrochemical etching of Ti sheets to produce heterostructured photocatalysts. Depending on the amounts of 3C-SiC nanocrystals on the TiO_2 nanotubes, photocatalytic degradation of organic species can be enhanced. The intrinsic electric field induced by the heterojunction promotes separation of the photoexcited electrons-holes in both the TiO_2 nanotubes and 3C-SiC nanocrystals. Hence, holes can more effectively travel to the surface of 3C-SiC nanocrystals and there are more electrons on the surface of TiO_2 nanotubes consequently forming more $^{\bullet}O_2^-$ and $^{\bullet}OH$ species to degrade organic molecules. © *2014 AIP Publishing LLC*. [http://dx.doi.org/10.1063/1.4882164]

3C-SiC nanocrystals (NCs) have attracted wide attention because they exhibit promising electronic and optical effects such as low dimensionality, quantum confinement, and shape effects.[1–5] Known for the chemical stability in photocatalytic processes,[1,6–8] nanostructured 3C-SiC has large potential in photoelectrochemical hydrogen production,[9] biological fluorescence labeling,[10] and intercellular pH monitoring.[11]

In composite semiconductor materials, an electric field is created at the heterojunction interface with matching band potentials and it enhances the transportation of photogenerated carriers between the composite materials and improves the photocatalytic efficiency due to efficient separation of the photoexcited electron-hole pairs.[12] Photocatalytic activity under UV irradiation has been observed from some SiC/TiO_2 photocatalysts[13–15] and it has been shown that in a dye-sensitized solar cell, the carrier recombination rate in a 3C-SiC/TiO_2 system is reduced.[16] However, the synthetic process is complicated and degradation of organic molecules by 3C-SiC NCs and TiO_2 nanotube (NT) heterostructures has not been reported so far. In this work, a simple method is adopted to synthesize the photocatalyst by direct incorporation of 3C-SiC NCs onto the TiO_2 NT array (NTA). Enhanced photocatalytic performance pertaining to organic species degradation is demonstrated and the mechanism is determined by microstructural and spectral characterization.

TiO_2 NTA was produced by electrochemical anodization of commercial titanium (Ti) foils (thickness: 0.25 mm, area: 5×2.5 cm^2, purity: 99.6%). All the chemical reagents were analytical grade and used without further purification. Before anodizing, the Ti foils were cleaned in acetone, ethanol, and distilled water ultrasonically for 30 min sequentially and dried in an oven. The electrolyte solution was prepared by dissolving NH_4F (0.5 wt. %) in a glycerol and water ($V_{glycerol}$:V_{water} = 17:3) solution. Anodization was performed on a two-electrode electrochemical cell with a Ti foil being the working electrode at a constant voltage of 50 V for 6 h similar to the procedures described in the literature.[17] After anodization, the samples were annealed in a tubular furnace in air at 450 °C for 2 h in order to improve the NTA crystallinity.[18]

The aqueous suspension containing the ultrathin 3C-SiC NCs was prepared with electroless etching.[19] In brief, 6.0 g of 3C-SiC powders with grain size of several micrometers were etched in a solution containing 15 ml of 65 wt. % nitric acid (HNO_3) and 45 ml of 40 wt. % hydrofluoric acid (HF) at 100 °C for 1 h. After cooling to room temperature, the solution was centrifuged at 8000 rpm for 5 min and then the precipitate was washed with deionized water. After drying at 70 °C for several hours, the sample was added to 30 ml of deionized water, followed by ultrasonic treatment for about 1 h (frequency: 40 kHz, power: 150 W). The solution was centrifuged at 8000 rpm for 10 min to obtain the supernatant containing 3C-SiC NCs. After equilibrating with NaOH, the supernatant was transferred to a dialysis bag and dialyzed against deionized water to remove residual acids and finally 25 ml of the neutral 3C-SiC NC solution was obtained.

To prepare the 3C-SiC-NC-decorated TiO_2 NTA, different volumes (0.25, 0.5, 1 ml) of the solution containing the 3C-SiC NCs were evenly drop-casted onto the fabricated TiO_2 NTA, followed by thermal treatment in an oven at 100 °C for 10 h. Afterwards, the TiO_2 NTA was washed with deionized water and dried at room temperature prior to the photocatalytic experiments. The photocatalytic measurements were performed at room temperature by monitoring the decomposition of methyl orange (MO) in the aqueous solution with a 440 W Xe lamp served as the light source. Typically, 20 ml of the MO aqueous solution (1 mg/l) and 80 ml of deionized water were put in a vessel and the photocatalytic films were placed in the solution for each test. Before each irradiation, the solution was magnetically stirred in darkness for 30 min to attain the adsorption-desorption equilibrium. During irradiation, 3 ml of the aqueous solution were extracted at 30 min intervals to determine the

a)Authors to whom correspondence should be addressed. Electronic addresses: hkxlwu@nju.edu.cn and paul.chu@cityu.edu.hk

concentration of MO from the absorbance change at a characteristic wavelength of 506 nm on an ultraviolet-visible (UV-vis) spectrophotometer.

X-ray photoelectron spectroscopy (XPS) was performed on a K-Alpha spectrometer (Thermo Fisher Scientific Corporation, USA) with Al K_α X-ray radiation and the resolution of the spectrometer was 0.1 eV. X-ray diffraction (XRD) was conducted on the X'PERT diffractometer (Philips Corporation, Holland). The microstructure and morphology were examined on a Hitachi-3400N scanning electron microscope (SEM, Hitachi Corporation, Japan) and high-resolution transmission electron microscope (HR-TEM, JEOL JEM-4000EX). The UV-vis absorption spectra were acquired on a UV-vis spectrophotometer (UV-2550, Shimadzu) and all the experiments were carried out at room temperature.

The morphology of the fabricated 3C-SiC NCs is similar to that observed previously.[2,9,20] They have a nearly spherical shape and the size is between 2 and 7 nm as shown in Fig. 1(a). The SEM image of the representative TiO_2 NTA is shown in Fig. 1(b). The NTs have a mean inner diameter of about 200 nm and the wall thickness is about 20 nm. The NT lengths are up to 5 μm (upper inset). After annealing at 450 °C, decoration with different amounts of 3C-SiC NCs, and photocatalytic experiments, the NTA morphology does not show obvious alteration (lower inset). This is because the amount of 3C-SiC NCs is very small and most of them are loaded on the internal wall of the tube, as shown in Fig. 1(c). The magnified HR-TEM image (inset) discloses the presence of 3C-SiC NCs. Here, it can be observed that the SiC NCs have not entirely covered the inner and outer surfaces of TiO_2 NTs and thus the partial NT wall can still make direct contact with organic molecules. The existence of 3C-SiC NCs is confirmed by XPS after photo-degradation further illustrating the good adhesion between 3C-SiC NCs and TiO_2 NTA and that separation of the NCs from the NT surface is difficult during degradation (the XPS spectra will be presented below).

The XRD patterns acquired from the 3C-SiC/TiO_2 NTAs are displayed in Fig. 2. For the NTA annealed at 450 °C in air for 2 h, three obvious peaks are observed at

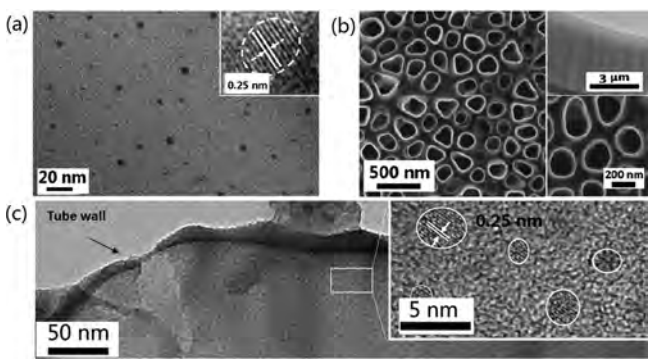

FIG. 1. (a) TEM image of the as-synthesized 3C-SiC NCs. The inset shows the magnified TEM image of one NC. (b) SEM images of the as-fabricated TiO_2 NTA and NTA annealed at 450 °C for 2 h decorated with 3C-SiC NCs (0.5 ml). The upper inset shows the lateral image of the NTA and the lower inset shows the NTA morphology after the photodegradation experiments. (c) TEM and HR-TEM (inset) images of 0.5 ml 3C-SiC NC-deposited TiO_2 NTA.

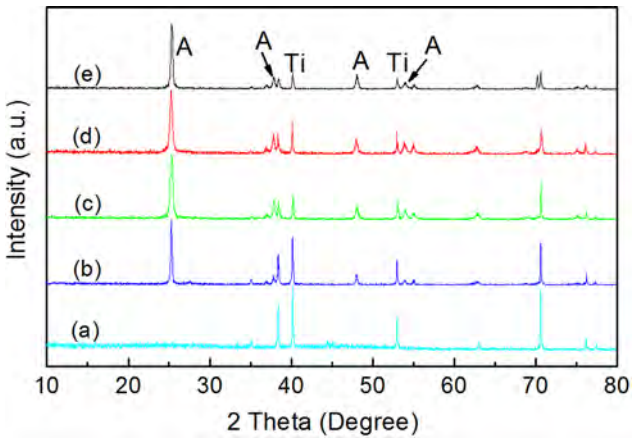

FIG. 2. XRD patterns: (a) As-prepared TiO_2 NTAs, (b) TiO_2 NTA annealed at 450 °C and drop-coated 0.25 (c), 0.5 (d), 1.0 (e) suspensions of 3C-SiC NCs. Label (A) stands for the anatase phase of TiO_2.

$2\theta = 25.2°$, 37.8°, and 48.1° [curve (b)]. They can be attributed to the crystalline phase of anatase TiO_2, indicating that the amorphous TiO_2 NTs crystallize during annealing. For the NTAs decorated with different amounts of SiC NCs, the XRD patterns hardly change and no diffraction peaks belonging to 3C-SiC NCs are observed[9] thus showing that there is only a small concentration of SiC NCs on the NTs.

The photocatalytic activity of the NTAs decorated with different amounts of 3C-SiC NCs is evaluated during vigorous stirring by Xe lamp irradiation. The results are shown in Fig. 3. In comparison, the control experiment shows no appreciable degradation in the case without the heterostructured photocatalyst (TiO_2 NTs/3C-SiC NCs) [curve (a)]. The pure TiO_2 NTA shows relatively low photocatalytic activity [only 45% degradation rate of MO after 3 h irradiation [curve (b)] and here the degradation rate is defined as $100\% \times (C_o - C)/C_o$]. This is due to the ultraviolet band gap of TiO_2 NTs only enabling absorption of a small content of ultraviolet light (4%). If we add the 3C-SiC NC suspension directly to the MO solution, no increased degradation is

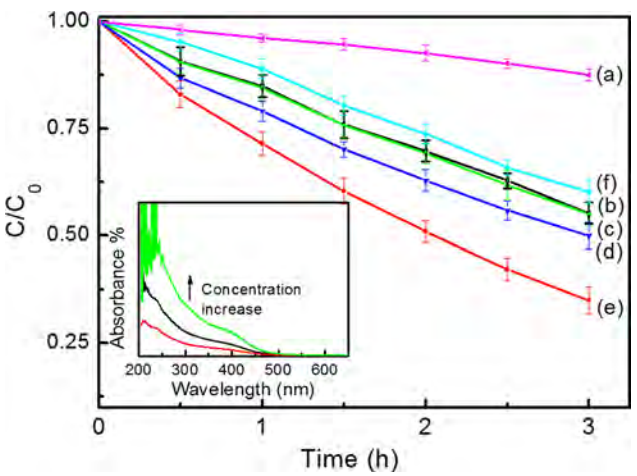

FIG. 3. Photocatalytic degradation of MO by the NTAs loaded with different amounts of 3C-SiC NCs: (a) self-degradation of MO, (b) NTA without 3C-SiC NC loading, (c) NTA with 0.5 ml 3C-SiC NC solution added in MO, (d) 0.25 ml 3C-SiC NCs/NTA, (e) 0.5 ml 3C-SiC NCs/NTA, and (f) 1.0 ml 3C-SiC NCs/NTA. The inset shows the UV-visible spectra obtained from the 3C-SiC aqueous solutions with different NC concentrations.

observed [curve (c)], indicating that high recombination rate of the photoexcited carriers in 3C-SiC NCs cannot lead to efficient MO degradation. After loading 0.25 ml of the 3C-SiC NC aqueous solution, the degradation performance on MO improves [curve (d)]. For the NTA decorated with 0.5 ml of the aqueous NC solution, the photocatalytic activity is largely enhanced [curve (e)], but further increasing the deposition volume to 1.0 ml decreases the photocatalytic activity. The degradation rate is smaller than that of pure TiO_2 NTA [curve (f)]. The largest photocatalytic rate is 65% when 0.5 ml of the 3C-SiC solution is loaded onto the NTA and the degradation activity is enhanced by 35%.

Figs. 4(a) and 4(b) show, respectively, the C 1 s and Si 2p core level XPS spectra of the NTA with 0.5 ml 3C-SiC aqueous solution after photocatalytic degradation. By means of XPS peak analysis, we can assign the origins of these peaks. For the C 1 s spectrum, the strongest fitted peak at 283.2 eV corresponds to SiC,[21,22] and the two small fitted peaks at 284.6 and 286.8 eV can be attributed to CH_n and O-CH_3 chemical bonds, respectively.[22,23] In the Si 2p spectrum, the strongest fitting peak stems from SiC, whereas the fitted peak at 100.7 eV can be assigned to the Si-OH.[20] The results corroborate the existence of 3C-SiC NCs on the TiO_2 NTA and indicate that the Si-terminated NC surface is connected to –OH. So the 3C-SiC NCs are hydrophilic[20] and benefit MO adsorption on the NCs/NTA photocatalyst.

Our measurements indicate that the 3C-SiC NCs and TiO_2 NTA are p- and n-type semiconductors, respectively. Thus, many PN junctions are formed at the interfaces between the 3C-SiC NCs and TiO_2 NT walls. As a result, there is an intrinsic electric field between the TiO_2 tube wall and 3C-SiC NC, as shown in Fig. 4(c). This electric field plays two roles. The first is to drive the photoexcited holes in the TiO_2 NTs to the SiC NC surface while keeping the electrons on the NTs. The second role is to effectively separate the photoexcited electrons and holes in the SiC NCs while keeping the holes on the 3C-SiC NCs. Meanwhile, the photoexcited electrons diffuse to TiO_2 NT walls. Hence, there are more electrons and holes to degrade MO. Since the photoexcited efficiency of the carriers is rather high in the 3C-SiC NCs,[24] the separated electrons and holes have high densities. In the heterostructure, the 3C-SiC NCs are not completely coated onto the TiO_2 NT walls. More electrons gather at the NT walls, whereas more holes accumulate on the 3C-SiC NCs because the conduction band (CB) and valence band (VB) of the 3C-SiC lie above the CB and VB of TiO_2 [Fig. 4(c)].[25,26] These holes react with -OH to form hydroxyl radicals ($^{\bullet}OH$).[20] Meanwhile, these electrons are trapped by the dissolved O_2 to form reactive oxygen species ($\bullet O_2^-$). The super oxide radicals ($\bullet O_2^-$) combined with H^+ form hydrogen peroxide (H_2O_2) and finally, H_2O_2 reacts with $\bullet O_2^-$ to form •OH, which is responsible for the enhanced degradation of the MO molecules.

When more SiC NCs cover the NTA, they will reduce the light absorption by the TiO_2 NTs. Since the 3C-SiC NCs are good light-emitting materials,[2,24] the radiative recombination rate of the photoexcited carriers is high. The absorbance of 3C-SiC increases with NC concentrations (inset in Fig. 3), and so the photocatalytic activity is reduced. This is the case for the 3C-SiC NCs/NTA heterostructure fabricated with 0.5 ml of the 3C-SiC NC aqueous solution on the NTA [curve (f) in Fig. 3].

In summary, different amounts of 3C-SiC NCs are loaded onto TiO_2 NTAs to construct heterostructures to enhance the photocatalytic activity. The heterostructure composite has higher photocatalytic ability pertaining to the removal of MO. The intrinsic electric field induced by the heterojunction promotes separation of photoexcited electrons and holes in both the TiO_2 NTs and 3C-SiC NCs, and more produced $^{\bullet}O_2^-$ and $^{\bullet}OH$ species make degradation of organic molecules more efficient. This study suggests the possible use of ultrathin 3C-SiC NCs as dopants to fabricate stable photocatalysts for degradation of organic species.

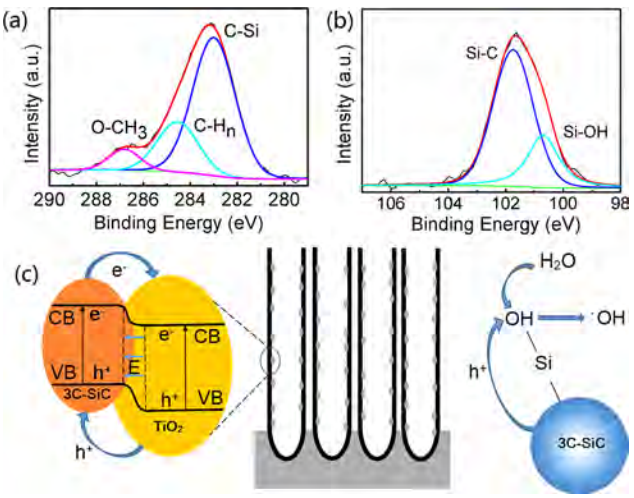

FIG. 4. XPS spectra: (a) Si 2p and (b) C 1 s core levels for the TiO_2 NTA decorated with 0.5 ml 3C-SiC NC suspension. (c) Schematic illustration of the band structure of 3C-SiC NC/TiO_2 NT heterostructure photocatalyst for charge transfer and separation under Xe light irradiation. $\mathbf{E}_{in}$ stands for the build-in electric field caused by p-n junction. Formation of $^{\bullet}OH$ radicals at the 3C-SiC NC surface is also plotted on the right side.

This work was supported by National Basic Research Programs of China under Grants (Nos. 2011CB922102 and 2014CB339800) and National Natural Science Foundation (No. 11374141). Partial support was provided by the Guangdong—Hong Kong Technology Cooperation Funding Scheme (TCFS) GHP/015/12SZ.

[1]M. J. Ledoux and C. P. Huu, CaTTech **5**, 226 (2001).
[2]X. L. Wu, J. Y. Fan, T. Qiu, G. G. Siu, and P. K. Chu, Phys. Rev. Lett. **94**, 026102 (2005).
[3]R. B. Wu, L. L. Wu, G. Y. Yang, Y. Pan, J. J. Chen, R. Zhai, and J. Lin, J. Phys. D: Appl. Phys. **40**, 3697 (2007).
[4]W. M. Zhou, X. Liu, and Y. F. Zhang, Appl. Phys. Lett. **89**, 223124 (2006).
[5]H. K. Seong, H. J. Choi, S. K. Lee, J. I. Lee, and D. J. Choi, Appl. Phys. Lett. **85**, 1256 (2004).
[6]Q. B. Ma, B. Kaiser, J. Ziegler, D. Fertig, and W. Jaegermann, J. Phys. D: Appl. Phys. **45**, 325101 (2012).
[7]Y. T. Gao, Y. Q. Wang, and Y. X. Wang, React. Kinet. Catal. Lett. **91**, 13 (2007).
[8]Q. B. Ma, B. Kaisera, and W. Jaegermann, J. Power Sources **253**, 41 (2014).
[9]C. Y. He, X. L. Wu, J. C. Shen, and P. K. Chu, Nano Lett. **12**, 1545 (2012).
[10]J. Y. Fan, H. X. Li, J. Jiang, L. K. Y. So, Y. W. Lam, and P. K. Chu, Small **4**, 1058 (2008).

[11]J. H. Guo, S. J. Xiong, X. L. Wu, J. C. Shen, and P. K. Chu, Biomaterials **34**, 9183 (2013).
[12]J. Su, X. X. Zou, G. D. Li, X. Wei, C. Yan, Y. N. Wang, J. Zhao, L. J. Zhou, and J. S. Chen, J. Phys. Chem. C **115**, 8064 (2011).
[13]H. Yamashita, Y. Nishida, S. Yuan, K. Mori, M. Narisawa, Y. Matsumura, T. Ohmichi, and I. Katayama, Catal. Today **120**, 163 (2007).
[14]N. Keller, V. Keller, E. Barraud, F. Garin, and M. J. Ledoux, J. Mater. Chem. **14**, 1887 (2004).
[15]D. Hao, Z. M. Yang, C. H. Jiang, and J. S. Zhang, J. Mater. Sci. Technol. **29**, 1074 (2013).
[16]Y. C. Lai and Y. C. Tsai, Chem. Commun. **48**, 6696 (2012).
[17]L. Jin, Z. W. Gao, J. Huai, X. Zhang, W. R. Guo, and L. Zhou, Chin. J. Funct. Mater. **43**, 2872 (2012).
[18]Y. Y. Zhang, X. L. Wu, L. Z. Liu, T. H. Li, and P. K. Chu, Appl. Phys. A **105**, 703 (2011).
[19]J. Zhu, Z. Liu, X. L. Wu, L. L. Xu, W. C. Zhang, and P. K. Chu, Nanotechnology **18**, 365603 (2007).
[20]X. L. Wu, S. J. Xiong, J. Zhu, J. Wang, J. C. Shen, and P. K. Chu, Nano Lett. **9**, 4053 (2009).
[21]M. Rosso, M. Giesbers, A. Arafat, K. Schroën, and H. Zuilhof, Langmuir **25**, 2172 (2009).
[22]K. H. Lee, S. K. Lee, and K. S. Jeon, Appl. Surf. Sci. **255**, 4414 (2009).
[23]M. Rosso, A. Arafat, K. Schroën, and M. Giesbers, Langmuir **24**, 4007 (2008).
[24]J. Wang, X. L. Wu, L. Z. Liu, and P. K. Chu, Scrip. Mater. **76**, 17 (2014).
[25]M. Grätzel, Nature **414**, 338 (2001).
[26]G. Mishra, K. M. Parida, and S. K. Singh, RSC Adv. **4**, 12918 (2014).